

Investigating the properties of supported vesicular layers on titanium dioxide by quartz crystal microbalance with dissipation measurements

Ilya Reviakine^{a)}

Department of Chemical Engineering, University of Houston, Houston, Texas 77204

Fernanda F. Rossetti

BioInterfaceGroup, Laboratory for Surface Science and Technology, Department of Materials, Swiss Federal Institute of Technology (ETH), Zurich, Switzerland

Alexander N. Morozov

Instituut—Lorentz for Theoretical Physics, Leiden University, Leiden, The Netherlands

Marcus Textor

BioInterfaceGroup, Laboratory for Surface Science and Technology, Department of Materials, Swiss Federal Institute of Technology (ETH), Zurich, Switzerland

(Received 22 March 2004; accepted 22 March 2005; published online 26 May 2005)

Adsorption of phospholipid vesicles on titanium dioxide was studied by a combination of quartz crystal microbalance with dissipation (QCM-D) and atomic force microscopy techniques. Vesicle size, concentration in solution, and bilayer composition were systematically varied. A strong dependence of the QCM-D response (magnitude of the frequency and dissipation factor shifts) on the vesicle concentration in solution was observed. QCM-D data were compared with a linear viscoelastic model based on the Voigt element to determine layer thickness, density, elastic modulus, and viscosity. Based on the results of this comparison, it is proposed that (i) layer thickness and density, as sensed by QCM-D, saturate much earlier (in time) than the actual surface coverage of the vesicles (number of vesicles per unit area); (ii) changes in surface coverage that occur after the density and thickness, as sensed by QCM-D, have saturated, are interpreted by the model as changes in the layer's viscoelastic properties. This is caused by the replacement of the viscous media (water) between the vesicles by viscoelastic media of similar density (vesicles); (iii) viscoelastic properties of layers formed at different vesicle concentrations differ significantly, while the vesicle surface coverage in those layers does not. Based on the comparison between the atomic force microscopy images and QCM-D data acquired at various vesicle concentrations it is proposed that QCM-D response is not directly related to the surface coverage of the vesicles. © 2005 American Institute of Physics. [DOI: 10.1063/1.1908500]

I. INTRODUCTION

Adsorption of intact vesicles to hydrophilic surfaces is the first step in the formation of supported phospholipid bilayers [SPBs (Refs. 1,2)].³⁻⁹ The transformation of the adsorbed vesicles into a SPB can proceed by at least two routes. The first route involves spontaneous rupture of individual surface-bound vesicles. It has been observed on mica and native silicon dioxide by atomic force microscopy (AFM),^{5,6} and on silicon dioxide films prepared by reactive sputtering by quartz crystal microbalance with dissipation measurement [QCM-D (Refs. 10,11)].⁸ The second route does not involve rupture of individual surface-bound vesicles. Instead, the vesicles accumulate on the surface, forming a supported vesicular layer, or SVL.¹² A SVL may be transformed into a SPB once a critical coverage of vesicles is reached,^{3-5,8} if Ca^{2+} is added to the preparation,^{5,12} or by some other stimulus.¹³ Under some conditions—a par-

ticular surface, lipid composition, absence of divalent cations, pH —a SVL appears to be the terminal structure that is formed, and no SPB formation is observed.^{5,12,14-17}

The pathway that is ultimately chosen by the vesicles depends on as of yet unknown details of vesicle-surface interactions. Some of the parameters that affect this process include surface charge, vesicle size and lipid composition of the bilayer, ionic strength, presence or absence of Ca^{2+} in the buffer. To understand the effect of these parameters on the process of bilayer formation, it is of interest to examine the properties of SVLs formed on surfaces under various conditions. The properties of interest include number of vesicles in the layer, the extent of vesicle deformation, and the rate at which this deformation occurs.

QCM-D, which has already significantly advanced our understanding of the SPB formation process,^{3,4,8,9,16-19} offers the possibility to assess quantitatively the properties of SVLs listed above. AFM, on the other hand, offers invaluable information concerning the organization of the surface-bound layers at nanometer length scales, and therefore provides information complementary to that provided by QCM-D. The combination of these two techniques has previously been

^{a)} Author to whom correspondence should be addressed; Present address: Institute of Physical Chemistry, Technical University Clausthal, Clausthal-Zellerfeld, D-38678 Germany; Electronic mail: ireviakine@uh.edu

successfully applied to the study of protein adsorption,²⁰ SPB formation,^{8,9,19} and other problems.^{21,22} In this study, it was used to examine the properties of SVLs formed on the surface of titanium dioxide as a function of vesicle size, bilayer composition, and vesicle concentration in solution. Vesicle size and bilayer bending modulus²³ (which is a function of bilayer composition and temperature) were chosen as variables because these are the two key thermodynamic parameters that govern vesicle behavior on a given surface,²⁴ while the concentration of vesicles in solution controls the kinetics of the adsorption process. A consistent, quantitative interpretation of the QCM-D and AFM data is arrived at, and assumptions implicit in previous QCM-D studies are scrutinized. In particular, it is conclusively demonstrated that QCM-D response cannot be directly interpreted in terms of the surface coverage of the vesicles.

II. EXPERIMENT

A. Substrate preparation and cleaning

Four inch silicon <110> wafers (Wafernet GmbH, Germany) used in AFM experiments and gold-coated quartz crystals for the QCM measurements (Q-Sense AG, Gothenburg, Sweden) were sputter coated with a 20 nm TiO₂ layer with a Leybold dc-magnetron Z600 sputtering plant as described previously.²⁵ Wafers were sawn into 10×10 mm² pieces on a wafer-sawing machine (ESEC, Zug, Switzerland). Immediately prior to each experiment, both types of substrates were cleaned by first incubating them in a 2% sodium dodecyl sulphate (Sigma, Buchs, Switzerland) solution for 30 min, rinsing with ultrapure water, and subjecting them to 30 min of UV/ozone treatment in a model 135 500 UV Cleaner from Boekel Industries Inc. (Feasterville, Pennsylvania) which was preheated for 30 min.

B. Vesicle preparation

Dioleoylphosphatidyl choline (DOPC) and dipalmitoylphosphatidyl choline (DPPC) were purchased from Avanti Polar Lipids (Alabaster, Alabama). Lipids were dissolved in chloroform, which was evaporated with an argon stream. The resulting lipidic film was further dried for 30 min in an oven (at room temperature) connected to an oil-free diaphragm-type vacuum pump. The dry film was resuspended in a buffer containing 10 mM HEPES, 2 mM ethylenediaminetetraacetic acid (EDTA), 100 mM NaCl, pH 7.4 (this buffer was used in all experiments described below unless stated otherwise; chemicals were purchased from Fluka Chemie GmbH, Buchs, Switzerland) to yield multilamellar vesicles (MLVs) at the desired concentration. Unilamellar vesicles (LUVs, for Large Unilamellar Vesicles) were prepared by extruding a suspension of MLVs through filters with pore diameters of 50, 100 or 200 nm using a Lipofast extruder (Avestin Inc., Canada). Vesicle solutions were stored under argon at +4 °C until used (no longer than 14 days). Vesicles (both MLVs and LUVs) made up of DOPC were prepared at room temperature, while those composed of DPPC were prepared at ~60 °C.

C. QCM-D measurements

QCM measurements were performed with a QCM-D QE301 (electronics unit)/QAFC301 (axial flow chamber)/QSoft 301 (software version) instrument from Q-Sense AB (Göteborg, Sweden).¹⁰ A TiO₂-coated crystal, cleaned as described above, was mounted in the instrument and checked for resonance on the first (base resonance frequency), third, fifth, and seventh overtones (the four overtones available on this instrument; crystals that would not resonate on one or more of these were not used). The chamber was filled with buffer and the instrument was allowed to equilibrate (while collecting data) until the drift in the frequency has settled out. The drift-free signal was collected for a further 10–30 min and is referred to as “base line.” Vesicle suspension of appropriate concentration was allowed to thermally equilibrate in the *T* loop of the instrument for 3 min and 0.5 ml of it was injected into the measurement chamber. Data were collected until the frequency signal stabilized. All measurements were performed at 25 °C. Only the data collected on the overtones were used for analysis. Data analysis was performed in Excel and MathCad according to the procedure outlined in Ref. 26 and consisted of fitting the data to the model described in Ref. 27 using layer thickness, density, viscosity, and elastic modulus as fitting parameters.

D. AFM measurements

Clean substrates were mounted on Teflon tape (BYTAC, Norton Performance Plastics Corporation, OH)-coated metal disks using double sided tape (after Mueller *et al.*²⁸), incubated with vesicle solutions of appropriate concentrations (between 0.004 mg/ml and 3 mg/ml) for 3–4 h in a humidity controlled chamber, and rinsed with buffer. AFM images were collected in buffer, in contact mode, with a Nanoscope IIIa MultiMode AFM (Veeco Metrology Group, Santa Barbara, CA) equipped with a “J” (120 μm) scanner, using oxide-sharpened silicon nitride tips mounted on cantilevers with a nominal force constant of 0.06 N/m, at an ambient temperature of ~22 °C. The fluid cell was washed extensively with a 2% sodium dodecyl sulfate solution and rinsed with ultrapure water before each experiment. *O* ring was not used. The microscope was allowed to equilibrate for a minimum of 30 min before imaging. Trace and retrace images were collected and compared. Images were flattened and plane-fitted as required.

III. RESULTS AND DISCUSSION

A. DOPC vesicles adsorb to the surface of titanium dioxide intact

When solutions of vesicles of various sizes (50, 100, 200 nm), composed of DOPC or DPPC, were allowed to interact with titanium dioxide-coated quartz crystals, frequency signal was observed to decrease, signifying the uptake of mass [Fig. 1(a)]. Simultaneously, the dissipation was observed to increase (Fig. 1(b)). Both signals were found to stabilize at a value (referred to as “the asymptotic shift”) that depended on vesicle size, bilayer composition, and vesicle concentration in solution. Previous studies have shown that this QCM-D

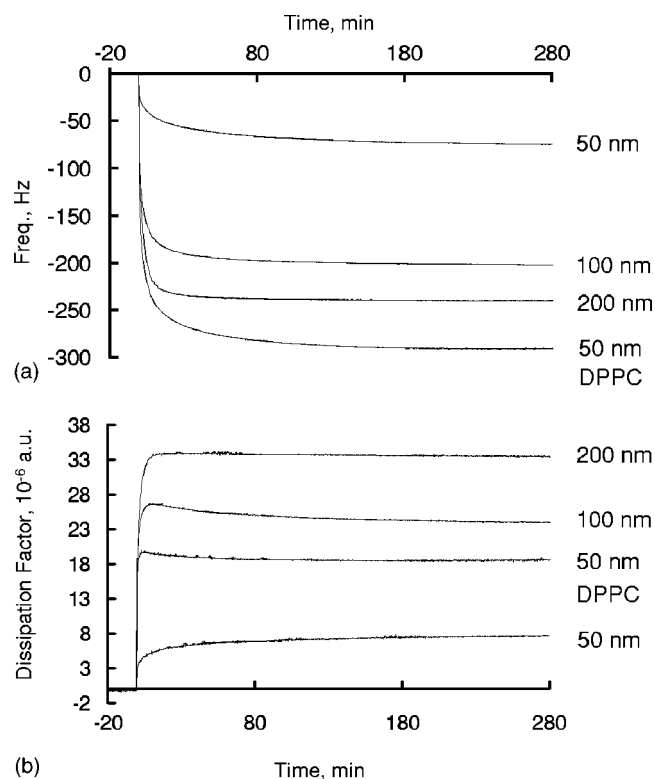


FIG. 1. Representative QCM-D curves for vesicles of various sizes and compositions adsorbing on TiO₂. In a typical QCM-D experiment, a crystal excited to oscillate at its resonance frequency and overtones in buffer was exposed to a solution of 50, 100, 200 nm DOPC or 50 nm DPPC vesicles in the same buffer. Frequency (top panel) and dissipation factor (bottom panel) were monitored on the third, fifth, and seventh overtones (~ 15 MHz, 25 MHz, and 35 MHz). In this figure, only the curves acquired on the third overtone are shown, and the frequencies are scaled by the overtone order. In general, adsorption of material is signified by a decrease in the frequency. The dissipation factor describes the ability of the layer to dissipate energy. Experiments shown in this figure were performed at the lipid concentrations of 0.4 mg/ml, 0.65 mg/ml, 0.52 mg/ml, and 0.65 mg/ml for the DOPC 50 nm, 100 nm, 200 nm, and DPPC 50 nm vesicles, respectively.

response [Fig. 1] is characteristic of the adsorption of intact vesicles and formation of SVL, rather than formation of supported bilayers.^{3,4} In that, our results are consistent with the previously reported findings by Reimhult *et al.*¹⁶

Intact vesicles were also observed on titanium oxide-coated surfaces exposed to vesicle solutions by AFM (Fig. 2). The size of adsorbed vesicles was measured as described previously⁵ and in all cases found to be consistent with the diameter of the pores through which the vesicle preparation was extruded, for example, for vesicles extruded through 200 nm pore diameter membranes, the size observed by AFM was 180 ± 40 nm (~ 200 vesicles measured), although a number of larger objects were also present. This is consistent with AFM observations reported by others.^{8,29} 400 nm DOPC vesicles were observed to adsorb to TiO₂ intact as well (not shown), but were not investigated further due to the significant polydispersity of the preparations.³⁰

Addition of Ca²⁺—a known fusogen^{31–33}—to the surface-adsorbed vesicles (at 2 mM concentration) failed to induce a transition to a supported bilayer (not shown). This stands in contrast to the ability of Ca²⁺ to induce supported bilayer formation from vesicles composed of zwitterionic phospholipids adsorbed on mica.⁵

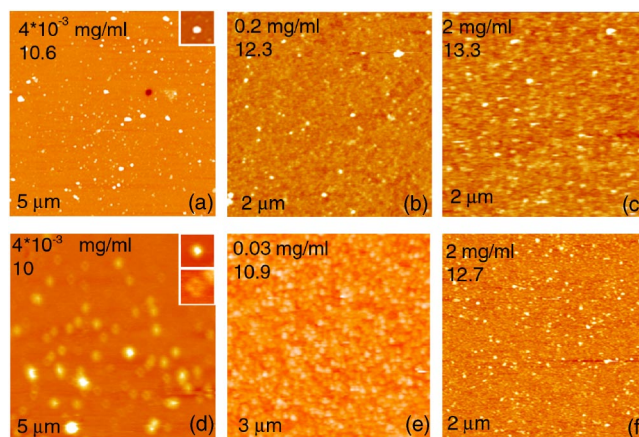


FIG. 2. Contact Mode AFM images of DOPC vesicles of various sizes adsorbed on TiO₂. (a)–(c) 100 nm DOPC vesicles, (d)–(f) 200 nm vesicles. Lipid concentration and \ln (vesicle concentration) are indicated in the top left corner of each image, while image size in the bottom left corner. Two kinds of objects can be discerned on the image of 200 nm vesicles taken at the lowest concentration (d): regular vesicles (top inset, 820×820 nm²) and objects of toroidal morphology (bottom inset, 410×410 nm²).

B. Asymptotic frequency and dissipation shifts depend on vesicle size, composition, and concentration in solution

In Fig. 3, the asymptotic frequency and dissipation shifts are plotted as a function of vesicle concentration³⁴ in solution. At high concentrations, the response of the QCM-D was independent of vesicle concentration and depended only on vesicle size and composition (Fig. 3). In this regime, larger vesicles were found to induce a stronger response. Stiffer DPPC vesicles [bilayer bending modulus $\sim 10^{-18}$ J (Ref. 35)] elicited a stronger response than their DOPC [bending modulus $\sim 10^{-20}$ J (Ref. 36)] counterparts of nominally the same size (50 nm): A frequency shift (third overtone, normalized to 5 MHz) of -280.8 ± 7.5 Hz (mean \pm standard deviation, six observations) was observed for the former, and -65.1 ± 18.5 Hz (eight observations) for the latter (Table I, Fig. 1). The time it took for the frequency signal to reach the plateau was similar for both the 50 nm DOPC and the 50 nm DPPC vesicles (Fig. 1), indicating that in solution, they had comparable sizes. Similar dissipation values observed for both kinds of vesicles [Fig. 1(b)] strongly suggest that in both cases, only a single monolayer of vesicles was formed. Therefore, QCM-D response is directly related to the properties of the SVLs that are affected by the different bilayer stiffnesses of the two kinds of vesicles (e.g., layer thickness²⁴).

At lower vesicle concentrations, the QCM-D response depended on vesicle concentration in solution (Fig. 3). Because a decrease in resonance frequency is normally taken to indicate an increase in the adsorbed mass at the crystal surface, it is tempting to directly interpret the observed dependence in terms of surface coverage of the vesicles. This would lead to a conclusion that SVLs prepared from solutions of different vesicle concentrations contain significantly different numbers of vesicles per unit area (the frequency shift changes by a factor of ~ 2 in the case of 100 nm vesicles and by a factor of ~ 6 in the case of 200 nm ones,

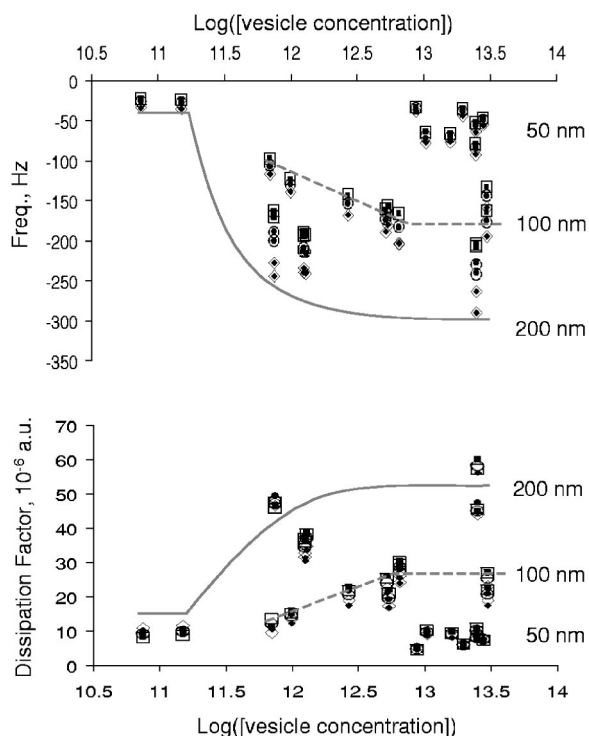


FIG. 3. Effect of vesicle size and concentration on QCM-D response. Asymptotic frequency shifts (top panel) and dissipation factor shifts (bottom panel) are plotted as a function of the logarithm of vesicle concentration (Ref. 34) for vesicles of various sizes. Data on all three overtones are shown, scaled by the overtone order: rhomb, third overtone; circle, fifth overtone, and square, seventh overtone. Filled symbols represent measured shifts, open symbols represent those calculated using the model of Voinova *et al.* (Ref. 27) as described in Reviakine *et al.* (Ref. 26) with layer density, thickness, viscosity, and elastic modulus as fitting parameters (Fig. 4). Lines are guides to the eye, and are used to indicate vesicles of which size were used in which experiments. The errors in the frequency [(observed - calculated)/observed \times 100%] were well below 1% of the frequency shift for most measurements, and in any case never greater than 2.2%. Errors in the dissipation factor were much larger and varied between 0.7% and (in one case) 19%, but on average were below 10% for the 50 nm vesicles, below 6% for the 100 nm ones, and below 5% for the 200 nm ones. This suggests that the model deals better with thicker viscoelastic films than with thinner ones, and may indicate that hydrodynamic contribution is more pronounced in the case of thinner inhomogeneous films.

Fig. 3). Yet two lines of evidence suggest that such an interpretation is, in fact, not correct: the dependence of the QCM-D response on vesicle concentration in solution *does not* directly reflect variations in the surface coverage of vesicles in the SVLs formed at different vesicle concentrations.

First, the results of the AFM experiments (Fig. 2) indicate that the surface coverage of vesicles does not undergo any dramatic changes over the concentration range where QCM-D response changes significantly (cf. Figs. 2 and 3) in the range between 0.03 mg/ml lipid and 0.4 mg/ml lipid, corresponding to \ln (vesicle concentration) of 10.9–12.0 for 200 nm vesicles, and of 11.5–12.6 for 100 nm vesicles, the frequency shift undergoes a change of ~ -240 Hz for 200 nm vesicles and of ~ -50 Hz for 100 nm vesicles. At the same time, the AFM images acquired at \ln (vesicle concentration) of 12.3 and 13.3 for 100 nm vesicles, 10.9 and 12.7 for 200 nm vesicles, are nearly identical, with the surface completely covered with the vesicles. (We further remark that at

0.03 mg/ml lipid, there are already ~ 10 times more vesicles (of either size) than is needed to cover the surface completely).

Second, the ΔF and ΔD vs \ln (vesicles concentration) curves shown in Fig. 3 do not extrapolate to zero. In fact, in the case of 100 nm vesicles, extrapolating the straight line portion of the curves shown in Fig. 3(a) to zero frequency shift yields a value of 10.2 for the \ln (vesicle concentration). Thus, according to this line of argument, no QCM-D response is expected at a vesicle concentration of $\sim 1.7 \times 10^{10}$ vesicles/ml (for 100 nm vesicles). This approximately equals the number of vesicles required to cover the surface of the crystal and experimental chamber completely. At the sensitivity of ~ 1 ng/cm², QCM-D is expected to be sensitive to 0.01%–0.04% of the maximum surface coverage (assuming it is sensitive only to the mass of the water inside the vesicles), or approximately between 2.2×10^5 and 1.1×10^7 vesicles/cm² (which is less than 1 vesicle/ μm^2).

If QCM-D response does not directly reflect the surface coverage of the vesicles in SVLs formed from solutions containing different vesicle concentrations, what does it reflect? To answer this question, the observed frequency and dissipation shifts were compared with predictions of a model using layer properties (mass, thickness, and viscoelastic properties) as fitting parameters. The results of this comparison, discussed in the next three sections, lead to a consistent interpretation of the dependence of QCM-D response on the concentration of vesicles in solution in terms of layer properties.

C. Interpretation of QCM-D data in terms of layer properties: The thickness of SVLs is independent of vesicle concentration in solution

Quantitative interpretation of QCM-D data in terms of layer properties (such as density and thickness) requires the use of a suitable model. Examples of available models include the one due to Sauerbrey,³⁷ which is useful for relating the frequency shift due to a thin, elastic, smooth, and nonporous layer to the layer's areal mass. None of these conditions are satisfied in the case of SVLs. More complicated models, ones that consider the contributions of the viscoelastic properties of the layer,^{27,38} and those which consider layer roughness (porosity) and the properties of fluid within the layer,³⁹ are also available. The former models include mass (the

TABLE I. Comparison between the SVLs composed of 50 nm DOPC and of 50 nm DPPC vesicles. The values are reported as average \pm standard deviation (number of observations). Since layer density was found to be independent of vesicle size, measurements with vesicles of all sizes were used to compute the average value. On the other hand, layer thickness depended on vesicle size, so only measurements done with 50 nm vesicles were used. Elastic modulus of 50 nm DOPC vesicles varied too much (around zero) for a reliable average value to be obtained.

Property	Bilayer composition	
	DOPC	DPPC
ρ (kg/m ³)	776 \pm 24(26)	850 \pm 5(9)
L (nm)	52 \pm 9(7)	83 \pm 3(6)
μ (N/m ²)	-	27 000 \pm 4000(3)
η (Ns/m ²)	(1.7 \pm 0.2) \times 10 ⁻³ (7)	(4.9 \pm 0.3) \times 10 ⁻³ (9)

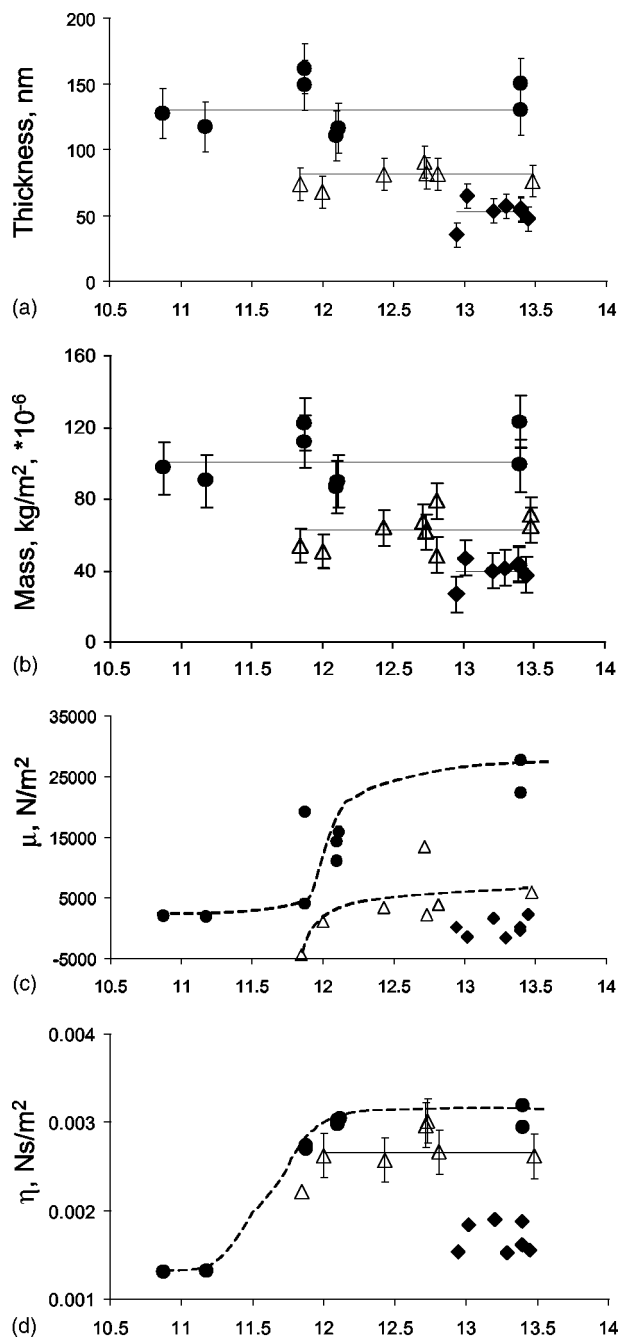


FIG. 4. Dependence of layer properties on vesicle concentration in solution. Layer thickness (a), mass [thickness \times density; layer density was found to be 776 ± 24 kg/m³ for DOPC vesicles of all sizes at all concentrations]; (b), elastic modulus μ (c), and viscosity η (d), obtained by fitting the asymptotic frequency and dissipation shifts shown in Fig. 3, are plotted as a function of the logarithm of the vesicle concentration. Filled circles, 200 nm vesicles; open triangles, 100 nm vesicles; filled rhombs, 50 nm vesicles. Solid lines in (a), (b), and (d) are averages of the respective values that are represented with symbols. Dashed lines are guides to the eye. The elastic modulus of the layer μ was found to vary significantly from experiment to experiment for the 50 nm vesicles, although the variation was around \sim zero and exhibited no systematic trends. In the case of 100 and 200 nm vesicles, systematic trends could be discerned for layer elastic modulus and, in the case of 200 nm vesicles, layer viscosity (dashed lines).

Sauerbrey term³⁷) and linear viscoelastic contributions. The latter can be readily extended to include the effects of adsorbed mass changes, but viscoelastic effects are neglected and are much more difficult to include.

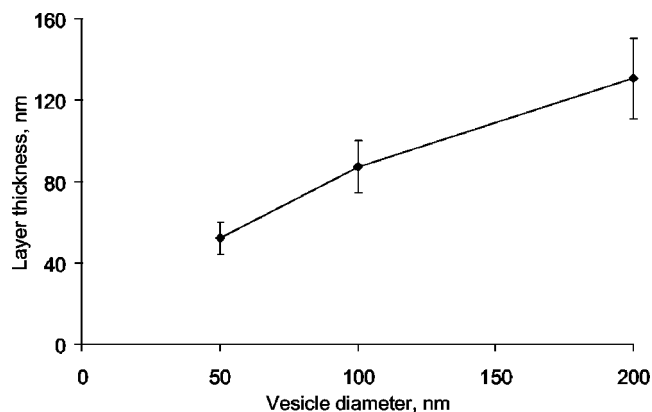


FIG. 5. Larger vesicles are deformed to a greater extent. The thickness of the SVLs is plotted against the diameter of the DOPC vesicles from which the SVLs were formed. While 50 nm vesicles do not appear to be deformed (i.e., the extent of their deformation is beyond the sensitivity of the technique), 200 nm vesicles are deformed to \sim 65% of their original size.

We have been unable to account for the QCM-D response observed with this system with a model which ignores viscoelastic properties of the layer. Therefore the model for a nonporous, smooth viscoelastic layer based on the Voight element was used.²⁷ Application of this model to our data, the results of which are shown in Figs. 3 and 4, demonstrates that within the scope of this model, the observed trends in the frequency and dissipation shifts are interpreted in terms of variations in viscoelastic properties of the layers, the density and thickness of which remain constant.

The fact that thickness of layers is unaffected by the concentration of vesicles in solution from which the SVLs were prepared implies that the rate of vesicle deformation is much higher than rate of adsorption at the highest of concentrations, i.e., SVLs are composed of deformed vesicles at all concentrations, and at all concentrations the vesicles of the same size are deformed to the same extent.

It is instructive to compare the thickness of the SVLs with the diameter of the vesicles from which they are formed to ascertain the extent of vesicle deformation. As expected, larger vesicles are deformed to a greater extent (Fig. 5). More detailed, quantitative analysis of the properties of SVLs will be presented separately.

D. The model adequately captures the mass uptake by the surface during the early stages of the adsorption process

During the initial stages of the adsorption process, QCM-D response must include changes due to the mass uptake at the surface. To verify that the model adequately captures this aspect of the adsorption process, we examined QCM-D response as a function of time at a given vesicle concentration (Fig. 6). Indeed, the model does reflect the mass uptake during early stages of vesicle adsorption [Fig. 6(c)], but the thickness and density of the layer saturate earlier than elastic modulus and viscosity [cf. Figs. 6(c), 6(d), 6(f), and 6(g)]. The changes in the viscoelastic properties which occur after the layer thickness and density have saturated cannot be interpreted in terms of vesicle deformation:

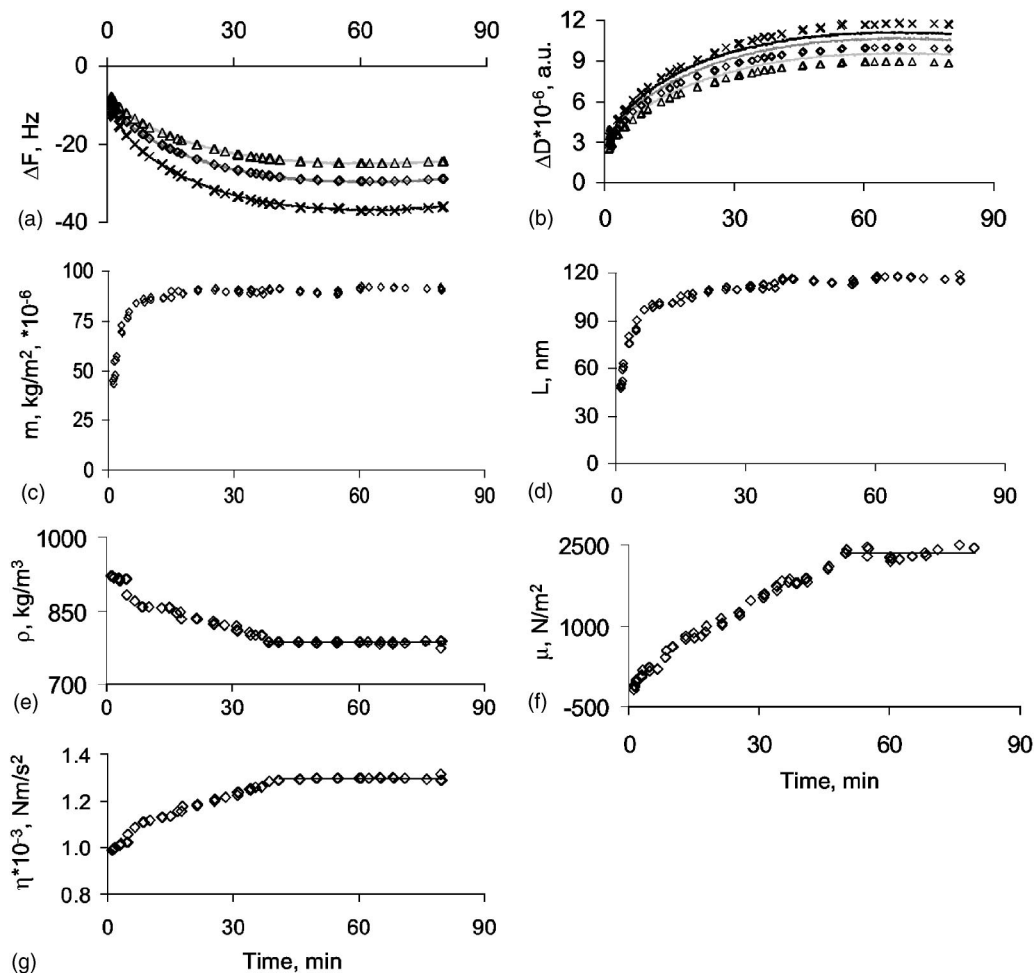


FIG. 6. Fitting the time evolution of the QCM-D response. Typical QCM-D curves showing the changes in frequency (a) and dissipation (b), relative to the bare crystal in buffer, upon injecting 200 nm DOPC vesicles at a lipid concentration of 0.06 mg/ml [vesicle concentration: $1.49 \times 10^{11} \ln(\text{vesicle concentration}):11.17$]. Black solid line/cross, third overtone; dark gray/rhomb, fifth overtone; and light gray/triangle, seventh overtone. Symbols are fits to the data, using layer thickness, density, elastic modulus, and viscosity as fitting parameters. The discrepancy between the observed dissipation values and those resulting from the fits in (b) are due to the fact that the dissipation of the bare crystal in vacuum is not taken into account in this model. See Ref. 26 for further discussion. The time evolution of adsorbed mass m , layer density ρ , thickness L , elastic modulus μ , and viscosity η , is shown in (c)–(g). Layer density (e) was observed to decrease from a value close to that of water to $785 \pm 3 \text{ kg/m}^3$ due to the increase in the volume fraction of the lipids within the layer as more vesicles adsorb (DOPC has a density smaller than that of water [$\sim 709 \text{ kg/m}^3$ (Ref. 44)]. This is lower than the density expected for undeformed 200 nm vesicles (830 kg/m^3). Deformation of the vesicles will result in a higher volume fraction of the lipids in the adsorbed layer as compared to the layer comprised of the undeformed vesicles even if the volume of individual vesicles does not change due to the deformation. (Thus, the assumption of constant layer density used in some of the previous studies to fit QCM-D data is not justified). Layer viscosity (f) is seen to increase approximately linearly from a value close to that of water to $(1.296 \pm 0.005) \times 10^{-3} \text{ Ns/m}^2$. Elastic modulus (g)—from \sim zero to $2400 \pm 120 \text{ N/m}^2$. At small times, negative values of elastic modulus are obtained from the model, implying that the model is not applicable to incompletely coated surfaces. Layer thickness saturates at $115 \pm 2 \text{ nm}$ and mass—at $9000 \pm 100 \text{ ng/cm}^2$. Straight lines indicate the portions of data which were used to compute average values of the appropriate quantities at saturation.

the latter also affects layer thickness, which was shown to remain constant while the viscoelastic properties continued to change (Fig. 6). The only remaining explanation is that continued adsorption of vesicles from solution alters the layer's viscoelastic properties without altering its thickness or density.

E. Addition of a small number of vesicles dramatically affects the viscoelastic properties of the layer: This is reflected in the QCM-D response

The interpretation of the QCM-D response arrived at in the two previous sections can be summarized as follows: After the surface coverage of vesicles has reached a certain value, the thickness of the layer and its density remain con-

stant (Figs. 4 and 6). Further adsorption of vesicles alters only the viscoelastic properties of the layer. This behavior can be understood in terms of the so-called “trapped solvent” hypothesis favored by the Chalmers group,^{11,40} also discussed in detail in Plunkett *et al.*⁴¹ Both are based on the observation by Martin *et al.*⁴² that solvent trapped between the surface features can be sensed as additional mass. (We would like to note that this interpretation may well be model specific, for instance, a consequence of model's ignoring the *changing surface roughness*³⁹ during adsorption, and slip (currently available models, including the one used here, had been derived using the no-slip boundary condition). These aspects have, to our knowledge, never been investigated).

It has been concluded earlier, based on the AFM obser-

vations and the analysis of the QCM-D response as a function of vesicle concentration in solution, that no significant changes in vesicle surface coverage occur in the regime where QCM-D response changes significantly (see Sec. III B). To reconcile this with the above interpretation, we propose that addition of a *small number* of vesicles to the layer can cause significant changes in the layer's viscoelastic properties. The difference in vesicle surface coverage can correspond, for example, to that between the random loose-packing limit (0.78) and random close-packing limit (RCP, 0.82), or RCP and the closed packed limit of 0.91,⁴³ in either case below 10%. To understand how such differences can affect the viscoelastic properties of a layer in a nonlinear fashion, it can be considered that at a lower surface coverage, there is still water between the vesicles, while at a higher coverage, the vesicles are in contact with each other. Thus, while a SVL formed at a low vesicle concentration will have a very similar number of vesicles per unit area to the one formed at a high concentration (Fig. 2), due to the effect the small difference in the number of vesicles per unit area has on the viscoelastic properties of the layers (Fig. 4), the two SVLs will evoke very different QCM-D responses (Figs. 3 and 4).

Two assumptions are implicit in this analysis: (i) that vesicles interact via excluded volume interactions only and (ii) that the surface-adsorbed vesicles are mobile. A consequence of this interpretation is that QCM-D response is not proportional to the surface coverage of the vesicles, but is either exaggerated by the influence the adsorbing vesicles have on the viscoelastic properties of the layer or understated due to the presence of the trapped solvent the adsorbing vesicles are replacing.

IV. CONCLUSIONS

Di-oleoyl and dipalmitoyl phosphatidylcholine vesicles of size 50–400 nm were found to adsorb to titanium dioxide surfaces intact, forming SVLs. Spontaneous formation of supported bilayers was not observed. Ca²⁺ failed to induce the transition to supported bilayers.

The properties of the SVLs were found to depend on vesicle size, bilayer composition, and concentration of vesicles in solution from which the layers were prepared. Consistent numerical values for layer density, thickness, shear elastic modulus, and viscosity could be obtained by comparing the frequency and dissipation shifts observed with QCM-D with a model in which the layer was represented by a Voigt viscoelastic element.

QCM-D response was found to be related not only to the surface coverage of the vesicles, but also, via the viscoelastic properties of the layer, to the interactions between them. Thus caution needs to be exercised when interpreting the QCM-D response in terms of surface coverage during adsorption processes.

ACKNOWLEDGMENTS

The authors wish to acknowledge Michael Horisberger (Paul Scherrer Institute, PSI, Villigen, Switzerland) for the sputter coating of the substrates; Dr. Susan M. DePaul

(Solvias AG, Basel, Switzerland), Dr. Ralf Richter (University of Bordeaux—1, Bordeaux, France Q-Sense AB, Göteborg, Sweden), Dr. Michael Rodahl (Q-Sense AB, Göteborg, Sweden), and Professor Diethelm Johannsmann (Technical University of Clausthal) for stimulating discussions. Furthermore, I.R. is grateful to Professor Peter Vekilov (University of Houston) for his support and for extending the invitation to A.N.M. to visit University of Houston. Financial support of the Swiss National Science Foundation under the R'Equip funding scheme to M.T. is also gratefully acknowledged.

¹H. M. McConnell, L. K. Tamm, and R. M. Weis, Proc. Natl. Acad. Sci. U.S.A. **81**, 3249 (1984).

²E. Sackmann, Science **271**, 43 (1996).

³C. A. Keller and B. Kasemo, Biophys. J. **75**, 1397 (1998).

⁴C. A. Keller, K. Glasmästar, V. P. Zhdanov, and B. Kasemo, Phys. Rev. Lett. **84**, 5443 (2000).

⁵I. Reviakine and A. Brisson, Langmuir **16**, 1806 (2000).

⁶J. Jass, T. Tjarnhage, and G. Puu, Biophys. J. **79**, 3153 (2000).

⁷J. M. Johnson, T. Ha, S. Chu, and S. G. Boxer, Biophys. J. **83**, 3371 (2002).

⁸R. Richter, A. Mukhopadhyay, and A. Brisson, Biophys. J. **85**, 3035 (2003).

⁹R. P. Richter and A. Brisson, Langmuir **19**, 1632 (2003).

¹⁰M. Rodahl, F. Höök, A. Krozer, P. Brzezinski, and B. Kasemo, Rev. Sci. Instrum. **66**, 3924 (1995).

¹¹M. Rodahl, F. Höök, C. Fredriksson, C. A. Keller, A. Krozer, P. Brzezinski, M. Voinova, and B. Kasemo, Faraday Discuss. **107**, 229 (1997).

¹²P. Nollert, H. Kliefer, and F. Jahnig, Biophys. J. **69**, 1447 (1995).

¹³A. Berquand, P. E. Mazeran, J. Pantigny, V. Proux-Delrouyre, J. M. Laval, and C. Bourdillon, Langmuir **19**, 1700 (2003).

¹⁴J. T. Groves, N. Ulman, P. S. Cremer, and S. G. Boxer, Langmuir **14**, 3347 (1998).

¹⁵P. S. Cremer and S. G. Boxer, J. Phys. Chem. B **103**, 2554 (1999).

¹⁶E. Reimhult, F. Höök, and B. Kasemo, Langmuir **19**, 1681 (2003).

¹⁷E. Reimhult, F. Höök, and B. Kasemo, J. Chem. Phys. **117**, 7401 (2002).

¹⁸E. Reimhult, F. Höök, and B. Kasemo, Phys. Rev. E **66**, 051905 (2002).

¹⁹R. P. Richter and A. Brisson, Langmuir **20**, 4609 (2004).

²⁰F. Caruso, D. N. Furlong, and P. Kingshott, J. Colloid Interface Sci. **186**, 129 (1997).

²¹I. Vikholm, T. Viitala, W. M. Albers, and J. Peltonen, Biochim. Biophys. Acta **1421**, 39 (1999).

²²B. Pignataro, C. Steinem, H. J. Galla, H. Fuchs, and A. Janshoff, Biophys. J. **78**, 487 (2000).

²³E. Sackmann, FEBS Lett. **346**, 3 (1994).

²⁴U. Seifert, Adv. Phys. **46**, 13 (1997).

²⁵R. Kurrat, M. Textor, J. J. Ramsden, P. Boni, and N. D. Spencer, Rev. Sci. Instrum. **68**, 2172 (1997).

²⁶I. Reviakine, A. N. Morozov, and F. F. Rossetti, J. Appl. Phys. **95**, 7712 (2004).

²⁷M. V. Voinova, M. Rodahl, M. Jonson, and B. Kasemo, Phys. Scr. **59**, 391 (1999).

²⁸D. J. Müller, M. Amrein, and A. Engel, J. Struct. Biol. **119**, 172 (1997).

²⁹H. Schonherr, J. M. Johnson, P. Lenz, C. W. Frank, and S. G. Boxer, Langmuir **20**, 11600 (2004).

³⁰N. Berger, A. Sachse, J. Bender, R. Schubert, and M. Brandl, Int. J. Pharm. **223**, 55 (2001).

³¹J. Wilschut, N. Duzgunes, and D. Papahadjopoulos, Biochemistry **20**, 3126 (1981).

³²N. Duzgunes, J. Paiement, K. B. Freeman, N. G. Lopez, J. Wilschut, and D. Papahadjopoulos, Biochemistry **23**, 3486 (1984).

³³E. P. Day, A. Y. W. Kwok, S. K. Hark, J. T. Ho, W. J. Vail, J. Bentz, and S. Nir, Proc. Natl. Acad. Sci. U.S.A. **77**, 4026 (1980).

³⁴Vesicles of different size will contain different numbers of lipid molecules. The difference is actually quite significant, as it scales with the square of the ratio between the radii of the vesicles: at a given lipid concentration, there will be 16 times more 50 nm vesicles than 200 nm ones. Therefore it is strictly speaking incorrect to compare results obtained at the similar lipid concentrations. The relevant quantity that needs to be considered is the vesicle concentration, which also determines the adsorption rate of the vesicles on the surface. It was calculated from lipid concentration using the molecular weight of the lipid [786.15 g/mol for DOPC (Ref. 45)] and

- area per lipid molecule [$0.82 \text{ nm}^2/\text{molecule}$ (Refs. 45,46)].
- ³⁵C. H. Lee, W. C. Lin, and J. P. Wang, *Phys. Rev. E* **64**, 020901 (2001).
- ³⁶G. Niggemann, M. Kummrow, and W. Helfrich, *J. Phys. II* **5**, 413 (1995).
- ³⁷G. Sauerbrey, *Z. Phys.* **155**, 206 (1959).
- ³⁸D. Johannsmann, *J. Appl. Phys.* **89**, 6356 (2001).
- ³⁹L. Daikhin and M. Urbakh, *Langmuir* **12**, 6354 (1996).
- ⁴⁰V. P. Zhdanov, C. A. Keller, K. Glasmästar, and B. Kasemo, *J. Chem. Phys.* **112**, 900 (2000).
- ⁴¹M. A. Plunkett, Z. H. Wang, M. W. Rutland, and D. Johannsmann, *Langmuir* **19**, 6837 (2003).
- ⁴²S. J. Martin, G. C. Frye, A. J. Ricco, and S. D. Senturia, *Anal. Chem.* **65**, 2910 (1993).
- ⁴³E. L. Hinrichsen, J. Feder, and T. Jossang, *Phys. Rev. A* **41**, 4199 (1990).
- ⁴⁴Lipid density was calculated from the area per molecule [$0.82 \text{ nm}^2/\text{molecule}$ for DOPC (Refs. 46 and 47)] and bilayer thickness at 20°C 4.51 nm for DOPC (Refs. 46 and 47).
- ⁴⁵P. L. Yeagle, *The Membranes of Cells*, 2nd ed. (Academic, San Francisco, CA, 1987).
- ⁴⁶D. Marsh, *Handbook of Lipid Bilayers* (CRC, Boca Raton, FL, 1990).
- ⁴⁷J. F. Nagle and S. Tristram-Nagle, *Biochim. Biophys. Acta* **1469**, 159 (2000).